



# Influence of Biochar on Unsaturated Hydraulic Characteristics of a Tropical Residual Silty Sand

Monir Hossain<sup>1</sup> · Apiniti Jotisankasa<sup>1</sup> · Surachet Aramrak<sup>2</sup> · Satoshi Nishimura<sup>3</sup> · Wanchai Yodsudyai<sup>1</sup>

Received: 16 December 2023 / Accepted: 4 August 2024  
© The Author(s), under exclusive licence to Springer Nature Switzerland AG 2024

## Abstract

Biochar-amended soil (BAS) is increasingly considered an effective cover material for various geotechnical and geo-environmental applications, owing to its potential to minimize infiltration, support vegetation and sequester carbon dioxide. However, the detailed hydraulic characterization of unsaturated tropical soil amended with biochar remains largely underexplored. This study investigated the hydraulic properties of residual silty sand (SM) amended with varying biochar contents (3.5, 5, 10, and 20% by weight) derived from corncob feedstock. This research focuses on crucial unsaturated soil parameters, including soil-water retention curves (SWRCs), saturated permeability ( $k_{sat}$ ) and permeability ( $k$ ) functions. The addition of biochar increased volumetric water content by 8–10% for suction ranges between 0 and 100 kPa compared to bare soil, due to the intraparticle voids and porosity of biochar. However, this effect was less pronounced with biochar percentages below 3.5%, especially for suctions below 5 kPa. The SWRCs of the BAS had bimodal shape with their fitting parameters nonlinearly increasing with biochar percentage. Biochar addition lead to notable reductions (about 20 times) in both saturated and unsaturated permeabilities, enhancement in suction stress and reduction in volume change upon drying. The implications of these observed behaviours were also discussed in terms of water holding capacity of biochar cover and environmental benefit in terms of CO<sub>2</sub> sequestration.

**Keywords** Biochar · Residual soil · Soil-water retention curves (SWRCs) · Permeability ( $k$ ) function · Suction stress · IPM · Soil cover · Soil-bioengineering · CO<sub>2</sub> reduction

## Introduction

Soil erosion stands as a serious threat in various geotechnical and geo-environmental structures, with far-reaching environmental consequences, including initiation of landslide, the loss of soil fertility, heightened pollution and sedimentation in water bodies, etc. [1–3]. Such erosion problem is intertwined with water infiltration and runoff phenomena that requires a holistic and nature-based solutions in geotechnics. Various types of innovative soil cover such as capillary barrier systems have gained considerable attention to prevent soil erosion and infiltration-related challenge in various geotechnical and geo-environmental applications with regard to bio-slope stabilization and waste disposal [3, 4]. Vegetation is a crucial part of such soil cover system which helps to prevent soil erosion and shallow slide through mechanical and hydrological reinforcement [5, 6]. Nevertheless, not all local soil types are suitable for the vegetation growth, and erosion may not be effectively arrested in the early stages of plant establishment. This is particular

✉ Apiniti Jotisankasa  
fengatj@ku.ac.th

Monir Hossain  
mdmonir.h@ku.ac.th

Surachet Aramrak  
agrscar@ku.ac.th

Satoshi Nishimura  
nishimura@eng.hokudai.ac.jp

Wanchai Yodsudyai  
fengwcy@ku.ac.th

<sup>1</sup> Department of Civil Engineering, Kasetsart University, Jatujak, Bangkok 10900, Thailand

<sup>2</sup> Department of Soil Science, Kasetsart University, Jatujak, Bangkok 10900, Thailand

<sup>3</sup> Division of Civil Engineering, Faculty of Engineering, Hokkaido University, Sapporo, Japan

so for tropical residual soils which, due to their high iron oxide content, are normally acidic and largely infertile, despite being considered as a reasonably good engineering soil. Biochar-amended soil (BAS) has been suggested for use in landfill cover material and soil improvement for agricultural practice [7–13]. Biochar is a stable, carbon-rich, porous material, which is made from renewable biomass, such as agricultural or forestry residues, within a controlled environment in the presence of little or no oxygen in a process called pyrolysis [14–16]. The addition of biochar to soil has been found to improve several physical properties for agricultural purposes, such as pore size distribution, porosity, bulk density, surface area, saturated hydraulic conductivity, and soil water retention capacity [7, 11, 13, 17–25]. Due to its high surface area, high pH value (alkaline), and high nutrient content, soil fertility can be greatly improved by addition of biochar. The oxidation process of methane ( $\text{CH}_4$ ) gas into carbon dioxide ( $\text{CO}_2$ ) can also be improved by adding biochar to landfill covers in order to minimize the emission of landfill gas [7, 14, 26, 27].

Several studies suggest that biochar can effectively store carbon in the soil for extended durations, exceeding 100 up to 4000 years [28–32], due to its predominantly condensed aromatic structure, which is highly resistant to microbial decomposition [33]. As a result, biochar effectively halts the emission of carbon dioxide ( $\text{CO}_2$ ) that would typically occur during the degradation of biomass. Wang et al. [34] and Sohi et al. [35] suggest that converting biomass to biochar can mitigate the worldwide environmental impact of landfill on climate change through carbon sequestration. According to Woolf et al. [36], the utilization of biochar and its incorporation into soil have the potential to decrease current human-caused  $\text{CO}_2$  emissions by as much as 12%.

The soil water retention curve (SWRC) and permeability ( $k$ ) function are important for evaluating climate-related soil behaviour in such geotechnical or geo-environmental engineering structures, such as landfill cover, capillary barrier systems, bioengineered slopes, and embankments, because they control the behaviour at hydraulic boundary conditions of unsaturated soil, such as infiltration, evaporation, etc. [3, 37–42]. SWRC provides the link between soil suction and water content which is in turn related to the soil's mechanical, hydraulic and thermal characteristics [43, 44]. Soil suction is one of the main stress variables used to describe the mechanical behavior of unsaturated soil [37]. In the characterization of soil in geotechnical or geo-environmental engineering discipline that involves unsaturated soil, the understanding of SWRC and permeability function is essential. The amendment of soil with biochar has the potential of altering the SWRC of the soil and suction stress [9, 45, 46]. For instance, the substantial specific surface area (SSA) of biochar is attributed to its high porosity, particularly the

existence of intraparticle pores inside the biochar structure. Especially, Lei & Zhang [46] revealed that the biochar addition considerably enhanced the formation of soil macroaggregates at the early incubation time. They also showed that saturated permeability of biochar-amended soils, especially those with biochars produced at high pyrolysis temperature, were higher than those without biochars on the sampling days. The feedstocks used to produce biochar play a crucial role in determining its properties. Treatments utilizing woodchip biochars resulted in higher saturated hydraulic conductivities compared to those using dairy manure biochar [46]. The intraparticle pores of biochars alters the distribution of pore sizes and the overall porosity in soil-biochar composites [14, 47–49]. The soil's capillary action can be affected by changes in pore size or porosity, thereby altering the SWRC [37, 50]. The wettability of biochar, namely its hydrophilic or hydrophobic properties, is influenced by the presence of surface functional groups such as carboxyl, hydroxyl, and phenolic groups. These features can also have an impact on the SWRC [26].

In recent years, extensive research has been done on how biochar affects the SWRC of agricultural soil in soil science discipline. The influence of biochar on tropical residual soil's SWRC is rarely studied in the context of geotechnical or geo-environmental applications [9, 11]. Notably, to the authors' knowledge, direct measurements of the permeability function of biochar-amended soils—specifically, the unsaturated permeability at different suctions—have not been reported in the literature. While this information is crucial for unsaturated seepage modeling, most previous studies on biochar have focused solely on saturated permeability. The effect of biochar on the SWRC of soil in geotechnical or geo-environmental engineering structures could also be different from that of agricultural soil due to various differences in soil traits such as density, soil formation, overburden stress, etc. [11, 17, 51, 52].

Therefore, the primary aim of this study is to investigate the influences of biochar on the hydraulic properties of unsaturated tropical soil, with a specific focus on soil-water retention curves (SWRCs), saturated permeability ( $k_{\text{sat}}$ ), and permeability ( $k$ ) function. The research tested residual silty sand (SM), collected from an erosion-prone slope in Northern Thailand, as the base soil, incorporating varying percentages of biochar (ranging from 3.5 to 20% by weight). Various mathematical expressions (newly developed and existing) are used to show the influence of biochar content on these unsaturated properties. This study extends its relevance to mechanical behavior by examining volume change behavior and predicting suction stress retention curves derived from SWRCs. Additionally, it demonstrates the application protocol of biochar, highlighting the benefits in

**Fig. 1** Highly eroded back slope at Highway No. 1192, Chiang Mai Province, Thailand, where the soil sample was taken



**Table 1** Basic properties of residual silty sand (SM)

Property	Test standard or method	Value
Liquid limit, LL (%)	ASTM D4318-10	39.8
Plastic limit, PL (%)	ASTM D4318-10	26.12
Plasticity index, PI	ASTM D4318-10	13.68
Standard Proctor compaction test		
Maximum dry unit weight (kN/m <sup>3</sup> )	ASTM D698-12	19
Optimum water content (%)	ASTM D698-12	11.0
Direct Shear test		
Cohesion, <i>c</i> (kN/m <sup>2</sup> )	ASTM D3080	6
Friction angle, $\phi'$ (degree)	ASTM D3081	27
Permeability Test (m./sec.)	ASTM D5084	2.41E-07

terms of water-holding capacity and carbon dioxide sequestration for a hypothetical soil cover.

## Materials and Methods

### Properties of Soil

The soil used in this study was classified as silty sand (SM). The samples were collected from a 45° cut slope at KM 11 + 500 (18°30'36.57" N, 98°25'50.18" E) of Highway No. 1192, Chiang Mai province, Northern part of Thailand. The geology of this area consists of granitic rock, which typically decomposes into silty and clayey sand (SM and SC). This residual soil is highly erodible (Fig. 1), as demonstrated by severe rills, sheets, and gullies in the area, that often lead to shallow (< 1 m deep) translational soil slides at the back slope along the route [4]. Soil samples were taken from the top soil layer (the upper 1 m) near the toe; then, they were air-dried, homogenized, and sieved (< 2 mm). The basic properties of soil are summarized in Table 1. Notably, this kind of sandy residual soil is typical of problematic soils found in the tropics where severe erosions and

shallow slides have become more increasingly frequent [39, 40, 43, 53]. By focusing on this representative soil type, a detailed understanding of biochar-soil amendment can be obtained which also serves as a foundation for future studies on other tropical soils.

The soil specimens (50 mm in diameter and 65 mm in height) were formed in one layer using static compaction method to reach the dry unit weight of 13.1 kN/m<sup>3</sup>, which represented the field condition of surface soil and equivalent to 69% of standard Proctor compaction. This loosely compacted state represents the commonly achievable dry unit weight of the soil fill placed inside the geocell compartment of a capillary barrier system in Thailand [4]. The suction of the bare soil sample was also measured using a miniature tensiometer and found to be above 90 kPa, corresponding to 11.4% of the gravimetric water content, which represented the average natural field condition prior to rainy season. PVC tubes were used to hold the samples for the hydraulic property tests as explained in the following.

Figure 2(a) displays the grain size distribution of both bare soil and biochar (corn cob). The bare soil comprises 1.8% gravel (> 4.75 mm), 58.2% sand (0.075 to 4.75 mm), 21.8% silt (0.005 to 0.075 mm), and 18.2% clay (< 0.005 mm). In contrast, if the biochar is classified with the ASTM standards, it primarily exhibits a gravel-sized composition. In Fig. 2(b), the effect of biochar amendment on the specific gravity of the soil is presented, where the specific gravity of bare soil and biochar is 2.69 and 1.48, respectively. The biochar content (*B<sub>c</sub>*) is defined as the ratio between biochar mass and bare soil mass, both in air-dried condition. Notably, the specific gravity of the soil decreases in the presence of biochar [3], suggesting biochar as a lighter material [3]. This trend is consistently observed across all biochar-amended soils (BAS).

**Fig. 2** (a) Grain size distribution of bare soil and biochar; (b) Specific gravity of BAS with various concentrations of biochar by weight ( $B_c$  equals biochar mass divided by soil mass)

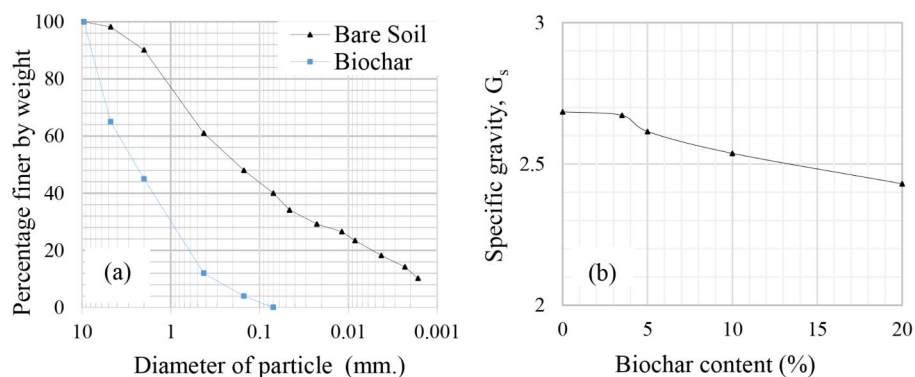


**Table 2** Physical and chemical properties of corncob biochar in this study

Description	Abbreviation	Biochar (Corncob)
Specific Gravity	$G_s$ (-)	1.48
Bulk Density	$\rho$ ( $\text{kN/m}^3$ )	4.36
pH	pH (1:10)	10.26
Electrical Conductivity	EC (1:5) (ds/m)	12.86
Organic Matter	OM (%)	26.42
Available Phosphorus	Aval. P (mg/kg)	3.173
Extractable Potassium	Ext. K (mg/kg)	29,984
Extractable Calcium	Ext. Ca (mg/kg)	891
Extractable Magnesium	Ext. Mg (mg/kg)	416
Extractable Sodium	Ext. Na (mg/kg)	54.01
Extractable Zinc	Ext. Zn (mg/kg)	0.34
Extractable Manganese	Ext. Mn (mg/kg)	4.06
Extractable Iron	Ext. Fe (mg/kg)	1.27
Extractable Copper	Ext. Cu (mg/kg)	0.15
Carbon-to-Nitrogen ratio	C/N ratio	18.59

## Properties of Biochar

The biochar in this study was produced from corncob feedstock using top-lit updraft (TLUD) technology [54, 55]. The TLUD technology is considered to have high thermal efficiency, ease of fuel ignition, low smoke emissions, and a higher biochar yield as compared to other technologies [54]. The corncob feedstock are residues from corn cultivation that are commonly disposed of through open-air burning by local farmers in Thailand and other parts of Southeast Asia, which leads to air pollution in the region. Thus, converting these corn cobs to biochar not only provides improvement in geotechnical soil cover, but also contributes to circular approach to the waste problem, improving carbon sequestration and air pollution reduction. The biochar specimen was obtained from Warm Heart foundation situated in Chiangmai province, Thailand which was typical of those producible from local farmers in Northern Thailand. Table 2 summarizes properties of the corncob biochar used in this study. With its alkaline pH of 10.26, biochar can help neutralize acidic conditions on slopes, enhancing vegetation

growth and ultimately increase the root reinforcement, and improve soil stability.

Furthermore, the high organic matter content, showcased at 26.42%, contributes to improved soil structure and moisture retention, a key advantage when implementing capillary systems for effective water distribution. As a soil cover, biochar forms a protective layer that not only conserves water but also promotes nutrient retention and microbial activity. Moreover, the scanning electron microscopy (SEM) images (Fig. 3) of biochar can help visualize its porous structure. All the images of corncob biochar showed highly porous morphology at 10, 20, 50 and 100  $\mu\text{m}$  with nearly rounded honeycomb surface, highlighting its potential to enhance capillary systems by facilitating water movement and root access, crucial for sustaining vegetation on slopes.

## FTIR-ATR Spectroscopy Analysis of Biochar

Fourier Transform Infrared (FTIR) spectroscopy results provide a qualitative description of the surface functional groups that are present in the biochar and soil. Figure 4 presents the FTIR-ATR (Attenuated Total Reflection) spectra of samples of corncob biochar and residual soil. In the figure, the ordinate represents the intensity of the absorption of a given wavelength in arbitrary units (a.u.). The specific chemical bond or functional group within the samples as determined through comparison with standard compound spectra [14].

The FTIR analysis results suggest that biochar contains a mixture of both hydrophilic and hydrophobic functional groups. The presence of hydrophilic functional groups (e.g., C-O at  $1000\text{ cm}^{-1}$ ) indicates that certain parts of the biochar may have an affinity for water, potentially making it effective for retaining moisture in soils. Conversely, the presence of hydrophobic aromatic carbon structures (e.g.,  $1400\text{ cm}^{-1}$ ,  $800\text{ cm}^{-1}$ ,  $700\text{ cm}^{-1}$ ) suggests that other components may repel water, making the biochar hydrophobic in some aspects.

The presence of small peaks in the 3700 and  $3600\text{ cm}^{-1}$  region, along with the high peaks in the region

**Fig. 3** Morphological scanning electron microscopy (SEM) images of various scales: (a) 10  $\mu\text{m}$ ; (b) 20  $\mu\text{m}$ ; (c) 50  $\mu\text{m}$ ; (d) 100  $\mu\text{m}$  of corncob biochar in this study

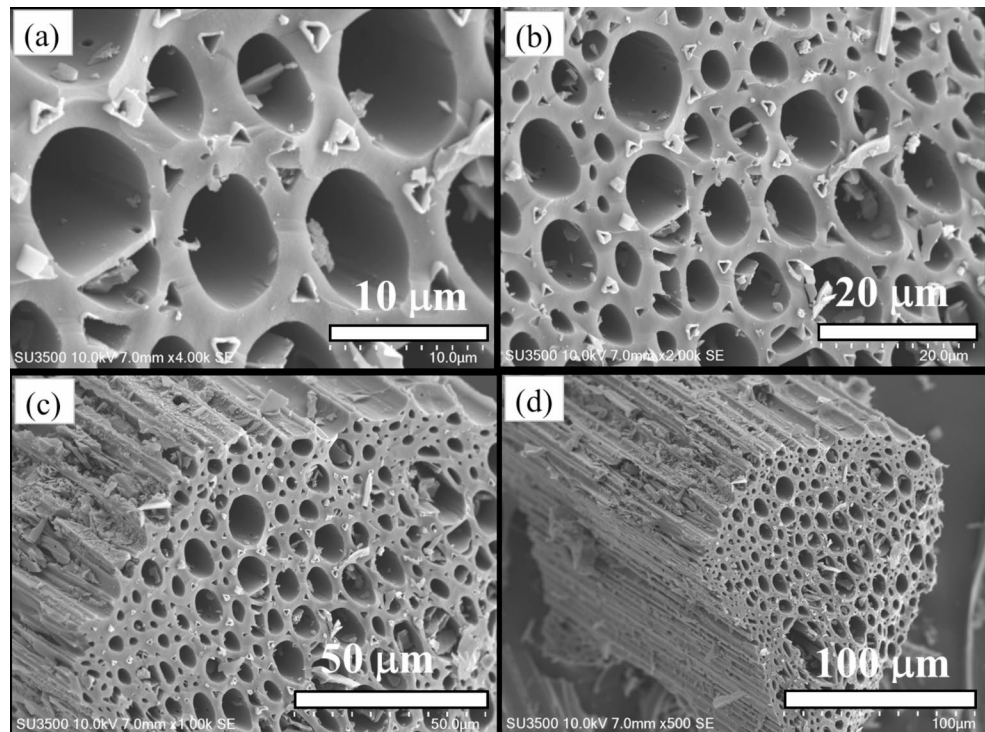
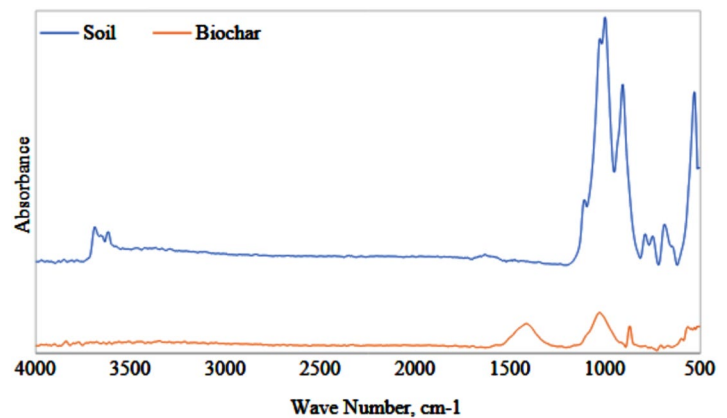


**Fig. 4** Surface functionality of corncob biochar and bare soil for this study



1000–1100  $\text{cm}^{-1}$  range, suggests that the soil contains hydrophilic functional groups (e.g., hydroxyls and amines) that can readily interact with water. On the other hand, the presence of peaks in the 1600  $\text{cm}^{-1}$  range, along with those in the 800, 700, and 500  $\text{cm}^{-1}$  range, indicates the presence of hydrophobic organic matter, possibly from nonpolar and aromatic compounds. This dual hydrophobicity/hydrophilicity could be beneficial for promoting plant growth, as hydrophilicity improves the water retention, while hydrophobic trait allows for soil aeration. Nevertheless, more studies are required to confirm this.

### Amendment Rate and Quantity of Biochar

The amendment rate of biochar does not only affect the soil fertility, but also influences soil hydraulic characteristics in

the geotechnical context [11, 56]. A low biochar amendment rate may not be enough to change the SWRC [11], while a higher rate may not be economically feasible or effective for large-scale applications, such as in bioengineered slopes and landfill covers. Therefore, the identification of optimum amendment rate is crucial for the effective utilization of biochar. Figure 5 shows the calculated rate of biochar amendment per unit area of soil slope ( $\text{kg}/\text{m}^2$ ) for various BAS cover thicknesses. The calculation was performed based on the typical field-observed dry unit weight of soil of 13.1  $\text{kN}/\text{m}^3$ . This kind of plot can be used for control of biochar application rate during construction of capillary barrier system. The rate of biochar per unit area can also be used to estimate the carbon dioxide sequestration as shown in subsequent section.

**Fig. 5** Amendment rate and quantity of biochar application determined for this study

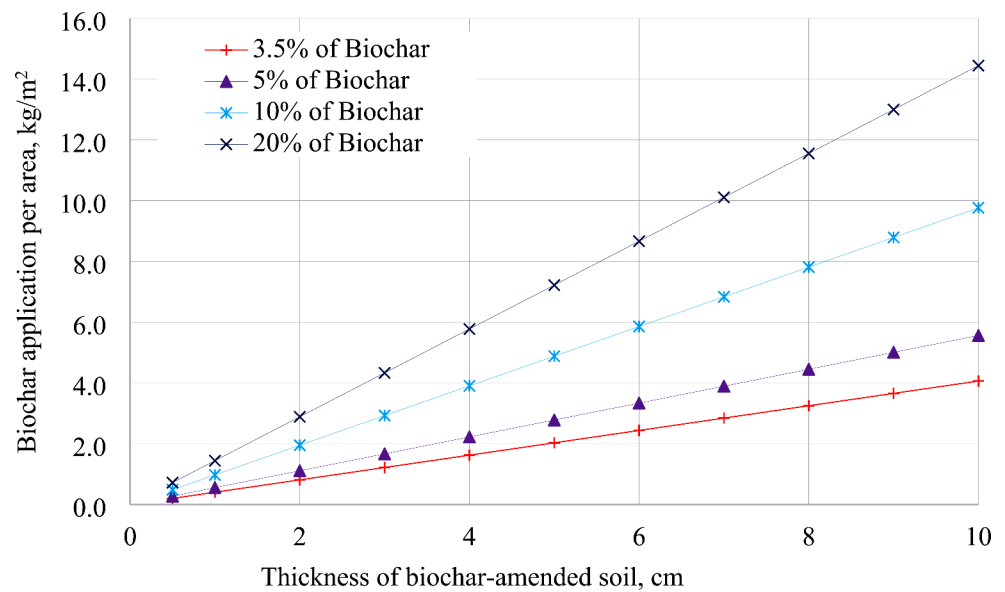
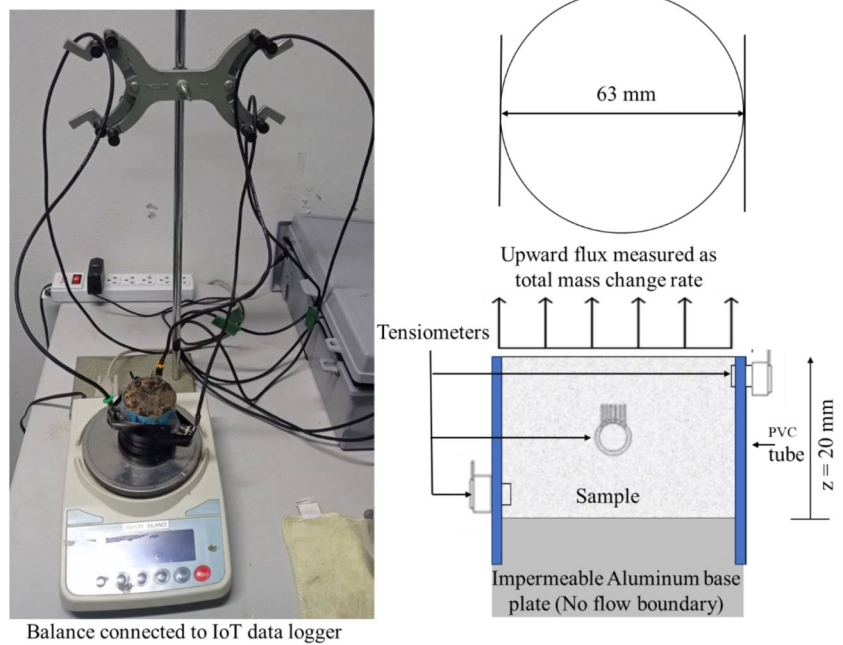


**Fig. 6** Instantaneous profile method (IPM) for drying test



## Testing Methods for Hydraulic Properties

In this study, the drying “instantaneous profile” (IP) method was used for measuring permeability of soils. This IP method is a typical transient-state testing method [42], which relies on continuous measurement of suction and mass (water content) gradient in order to obtain an unsaturated permeability function [53, 57]. The IP technique adopted in this study employ tensiometers for suction measurement along the sample which was continuously weighed for mass change during drying from the upper face [53, 57, 58]. The test program involved first soaking the sample in water for about 4 days before the drying IP test, whereby soil suction

increased from 0 to about 100 kPa at the end of testing. After the completion of the IP test, the sample was re-soaked for 4 days prior to the saturated permeability test.

The experimental setup of the drying IP test in this study is shown in Fig. 6. This setup was similar to the simplified evaporation IP method proposed by Peters and Durner [59] and Jotisankasa and Sirirattanachai [43]. The top surface of the soil sample was exposed to ambient air, inducing a controlled one-dimensional upward flow of moisture due to evaporation. The sample’s base was underlain by an impermeable solid plate. Typical results of a drying IP test are shown in Fig. 7. Profiles of soil suction were monitored continuously using miniature tensiometers [58] at three

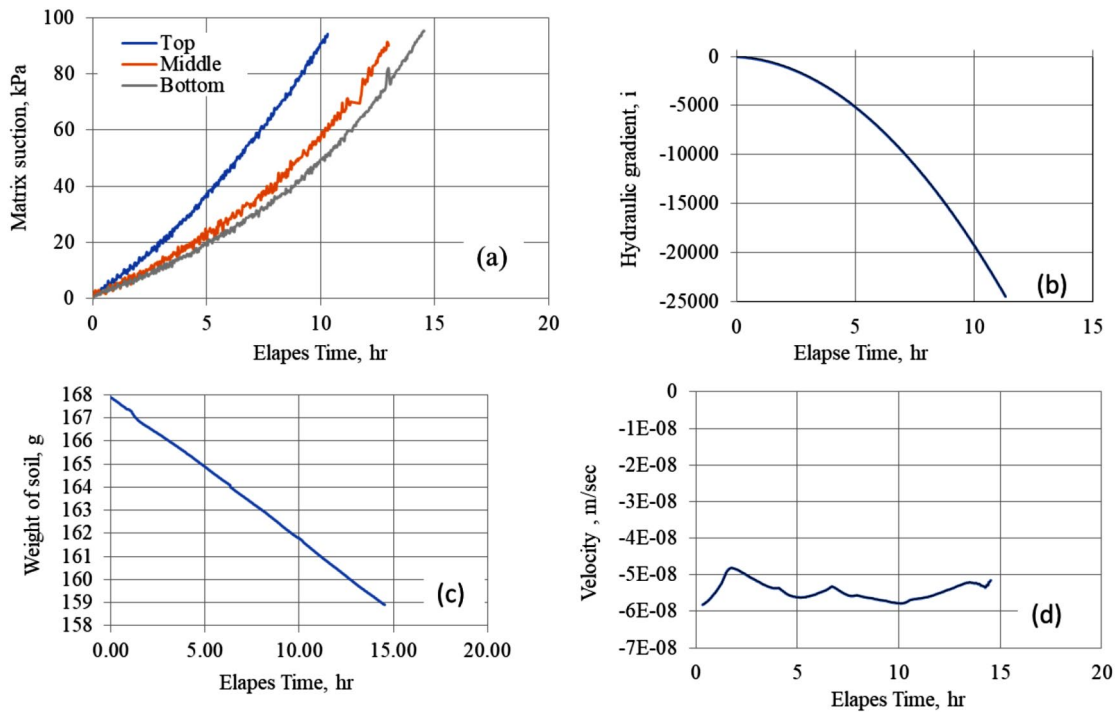


**Fig. 7** Typical test result of drying IP test (Biochar 3.5% (w/w) of air-died soil): (a) matric suction versus time; (b) hydraulic gradient versus time; (c) change of soil mass versus time; (d) discharge velocity versus time

locations on the sample’s side, as shown in Fig. 6 and the typical result in Fig. 7a, following the calibration process with an accuracy of  $\pm 0.15$  kPa. Additionally, a data-logging balance with a precision of 0.01 g was utilized to continuously measure the weight of the soil sample, as shown in Fig. 6, facilitating the calculation of the total moisture flow rate across the sample. It is noted the range of maximum suction measurement during IP test was only limited to 100 kPa. This range of suction is important for slope application as observed in our previous field measurements on silty sand slopes in rainy seasons, e.g. Jotisankasa et al. [60]; Jotisankasa, and Mairaing, [61]

The hydraulic gradient,  $i$ , was determined by utilizing the suction values obtained from three different locations, as follows:

$$i = \frac{d[h_e - (\frac{\psi}{\gamma_w})]}{dz} \tag{1}$$

where  $h_e$  is the elevation head at each tensiometer location,  $\psi$  is the matric suction,  $\gamma_w$  is the unit weight of water, and  $z$  is the elevation. The hydraulic gradient value,  $i$ , shown in Fig. 7b, was calculated by using linear regression on the three suction readings.

The discharge velocity,  $v$ , at any given time was calculated as shown in Fig. 7d, as follows:

$$v = \frac{dV_w}{Adt} \tag{2}$$

The change in volume of water in the soil sample, denoted as  $dV_w$ , is determined by measuring the change in soil mass throughout testing, as seen in Fig. 7c.  $A$  represents the cross-sectional area of the sample, while  $t$  represents the elapsed time. Darcy’s law can be employed to calculate the permeability value at any given suction and volumetric water content.

$$k = \frac{v}{i} \tag{3}$$

### Suction Measurement

There are a variety of methods for measurement of matric suction such as axis translation, tensiometer, filter paper etc. [37, 53, 62]. A small tensiometer with microelectromechanical system (MEMs) pressure sensor, 1BAR High-Air-Entry porous ceramic, and transparent acrylic tube developed by Kasetsart University (KU) was used in this study (Fig. 8a&b). The pointwise method involves taking measurements of soil suction at various moisture levels. A minimum of 2–3 days was given between each step of increase in soil suction. The compacted sample in the pointwise SWRC experiments had

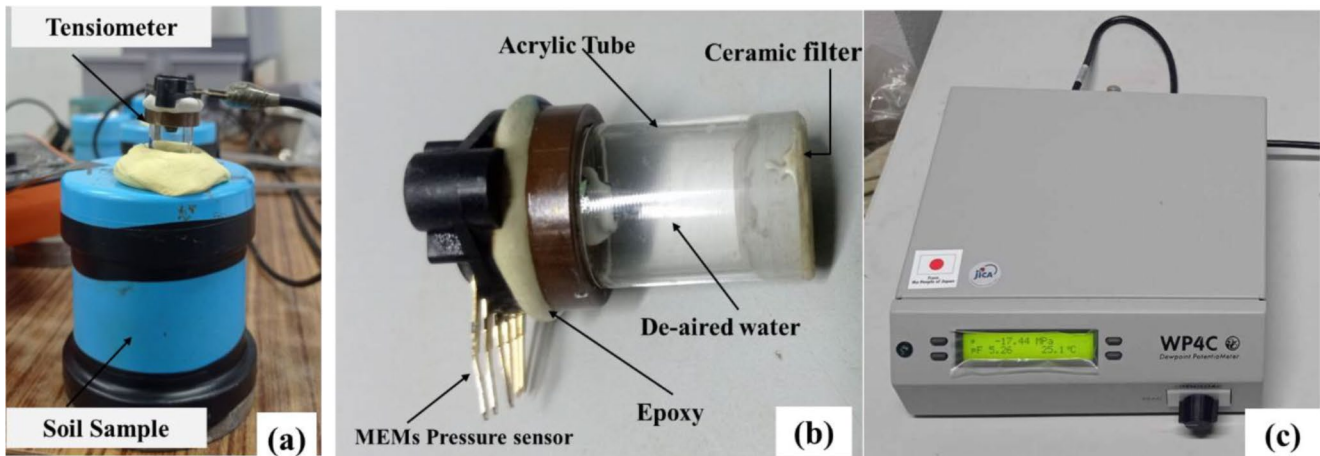
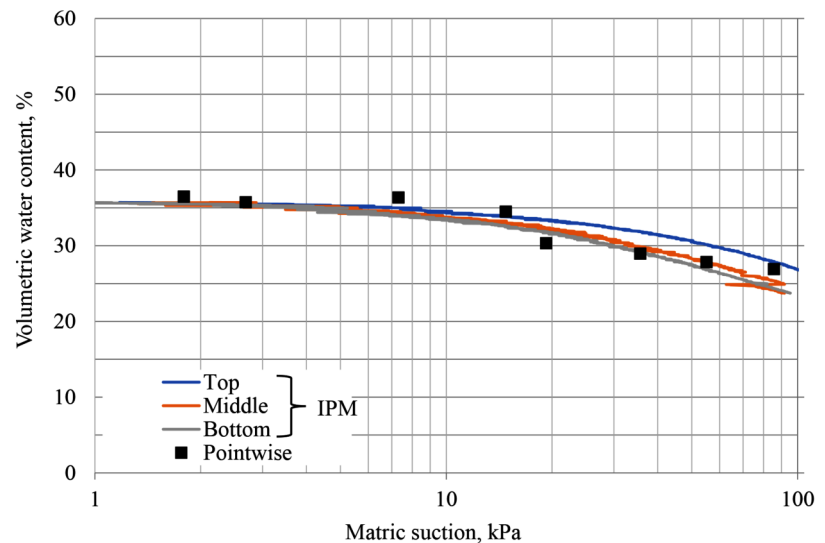


**Fig. 8** Experimental setup and equipments used (a) pointwise measurement of matric suction on a sealed sample (b) miniature KU-tensiometer and (c) WP4C potentiometer for total suction measurement

**Fig. 9** SWRCs from IP drying tests and point-wise testing performed on samples of silty sand (SM) with 3.5% biochar



the same diameter of 63 mm as the drying IP specimens with an average height of 23.5 mm. Typical results of matric suction measured by the KU-tensiometer, using the pointwise and continuous method (IP-Instantaneous profile), are shown in Fig. 9. A good agreement was observed between the two kinds of tests, indicating the reliability of the IPM method in determining the relationship between volumetric water content and matric suction. Among the curves examined, the middle curve exhibits the best fit with the pointwise data, as demonstrated by the lowest Root Mean Square Error (RMSE) of 1.67% and the highest coefficient of determination ( $R^2$ ) value of 0.829. This suggests that the middle curve most accurately represents the relationship between volumetric water content and matric suction. The bottom curve also shows a strong correlation with the pointwise data, although it is slightly less precise than the middle curve, with an RMSE of 1.80% and an  $R^2$  value of 0.805,

indicating a reliable but slightly less accurate fit. The top curve, while still in good agreement, is less precise than the other two curves, with an RMSE of 1.83% and an  $R^2$  value of 0.720.

This study also relied on the WP4C potentiometer (Fig. 8c) for measuring total suction beyond 500 kPa in soil specimens. It is noted that separate samples (measured 3.75 cm in diameter and 0.8 cm in height), of similar density to specimens in other suction tests, were used in the WP4C total suction measurement. The method, outlined in previous works by Fredlund et al. [63], Rahardjo et al. [41], and Jotisankasa et al. [4], involves thermodynamically equilibrating the soil specimen in a temperature-controlled chamber. The chamber is sealed for precision, and a Peltier cooling device cools a mirror to its dew-point temperature. Condensation onset is detected using a photoelectric sensor, while an infrared thermometer measures chamber temperature. This



method yields essential data, including both saturated and above-specimen water vapor pressures, which can then be used to calculate total suction and determine the SWRC in higher suction range (> 500 kPa).

## Results and Discussion

### Effects of Biochar on Saturated Permeability

The variation of saturated permeability with biochar percentage is shown in Fig. 10. There is a noticeable decrease in saturated permeability ( $k_{sat}$ ) as the biochar content in the soil increases to 0.035 (3.5%) and its effect seemed to level off as the biochar amount increased further. This is an important finding because it signifies that optimal biochar addition in soil cover that can retard the water infiltration into the underlying soil. In this study, a new mathematical expression (Eq. 4) was proposed to model the variation of saturated permeability with biochar content as follows.

$$\frac{k_{sat}}{k_{sat,o}} = \exp\left(\frac{Bc}{a + (b \times Bc)}\right) \tag{4}$$

In this equation, the saturated permeability of BAS ( $k_{sat}$ ) is normalized by that of bare soil ( $k_{sat,o}$ ) and related with the biochar content ( $Bc$ ). The two parameters,  $a$  and  $b$ , are the soil constants ( $a=0.00198$ ,  $b=0.32204$ ) that capture how changes in  $Bc$  influence permeability and were calculated using Microsoft Excel Solver to obtain the minimum value of root mean square error of  $\ln\left(\frac{k_{sat}}{k_{sat,o}}\right)$  (RMSE=0.017), yielding the  $R^2$  value of 0.9998. The  $a$ -parameter determines the point at which the influence of  $Bc$  on permeability becomes significant, while the  $b$  parameter regulates the rate of change in permeability concerning biochar ( $Bc$ ). Biochar is known for its porous structure [17, 25], which can help retain water and nutrients, thus improving the ecological value of slope. It is quite interesting to observe that this porous material can also reduce the soil permeability. The highest percentage of

biochar in the study, which is 20%, resulted in the lowest saturated permeability,  $k_{sat}$ , at 1.187E-08 m/sec.

Since the soil-biochar mixture is composed of the silty sand and lighter biochar particles, the biochar would occupy more space than the silty sand particles of the same weight, given the biochar's lower specific gravity. Provided that all the BAS samples were compacted to the same dry unit weight as the bare soil, the silty sand particles in BAS would need to be squeezed into a smaller volume than those in the bare soil. Therefore the silty sand parts in BAS would be of higher density than the bare soil. Understandably, the denser sand matrix with biochar inclusion is expected to be of lower permeability than the bare soil, despite the fact that the whole mixture of BAS was compacted to the same unit weight. This finding is particularly interesting for such applications as landfill cover and bioengineered embankment and cut slope, which have simultaneous requirements of controlling water infiltration and retaining moisture for plant growth in the upper soil layer. Traditional low permeability soil covers used in geotechnical engineering, like compacted clay or soil-cement mixture, in the other hands, are normally too dense to facilitate plant growth or to provide ecological services for slope. These traditional soil covers are constructed with processes that induced carbon emissions while the biochar helps to offset carbon. As more emphasis is placed on low carbon design in geotechnics, this information is particularly useful to accelerate carbon neutrality in our discipline.

### Effects of Biochar on SWRCs

#### Lower Suction Range

In Fig. 11, soil-water retention curves (SWRCs) for the silty sand (SM) in a suction range lower than 100 kPa (matric suction range) are depicted under different biochar content conditions (3.5%, 5%, 10%, and 20% by weight). These curves were calculated, as was previously stated, from middle tensiometer suction measurements, which were taken to

**Fig. 10** Correlation between biochar content and the saturated permeability of biochar amended soil

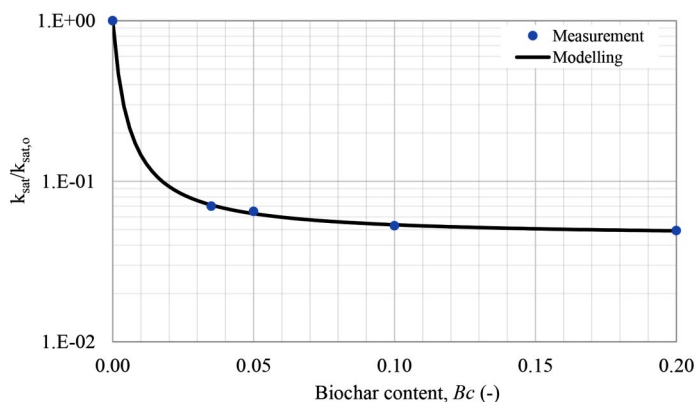


**Fig. 11** Soil-water retention curve (SWRC) of clay sand fitted to the van Genuchten equation for biochar amended soil

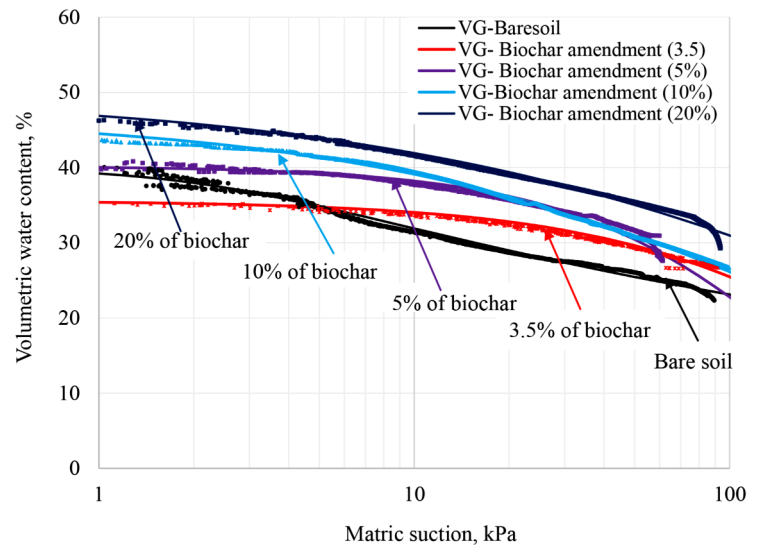


**Table 3** Van Genuchten equation fitting parameters for biochar amendment soil for matric suction

Description	Symbols	Concentrations of biochar with silty sand (SM) by weight				
		0**	3.5%	5%	10%	20%
Model parameter close to air-entry value (AEV), kPa <sup>^</sup>	$\alpha$	0.322	0.021	0.026	0.093	0.101
Model Parameter	$n$	1.191	1.400	1.537	1.250	1.212
Saturated volumetric water content, %	$\theta_s$	40.000	35.000	39.649	44.062	47.000
Residual volumetric water content, %	$\theta_r$	5.000	5.000	5.000	4.000	5.000
Coefficient of determination	$R^2$	0.990	0.883	0.975	0.999	0.978

0\*\* = Control (Bare soil), Model parameter,  $m = (1-1/n)$

reflect typical suction levels. The curve fitting models using van Genuchten [64] (see Eq. (5)) is also shown in Fig. 11 and the fitting parameters are summarized in Table 3;

$$\theta = (\theta_s - \theta_r) \left[ \frac{1}{1 + (\alpha \cdot \psi)^n} \right]^m + \theta_r \tag{5}$$

;where,  $\theta$  is the volumetric water content (%);  $\psi$  is the soil suction;  $\theta_s$  and  $\theta_r$  saturated and residual volumetric water content;  $\alpha$  is the empirical scale parameter; and  $n$  and  $m$  are the curve shape factor which controls the slope of the SWRC ( $m = 1 - (\frac{1}{n})$ ). The van Genuchten model, widely used in geotechnical engineering, soil science and hydrology, offers a valuable representation of the soil water retention curve in unsaturated soils, and simplifies the relationship between soil water content and soil water potential. To determine the fitting parameters ( $\alpha$ ,  $m$  and  $n$ ), a graphical method can be used but often considered to be subjective and time-consuming [65]. In this study, a solver function in Excel was utilized to vary the fitting parameters until the minimum value of root mean squared error (RMSE) was obtained. Nevertheless, the equation may still not always be suitable to capture the bio-modality in SWRC as will be explained thereafter.

**Entire Suction Range**

Figure 12, representing soil water retention curves (SWRCs) and curve-fittings based on Gitirana and Fredlund’s equation, over the entire range of matric and total suctions. The curve fitting parameters using Gitirana and Fredlund [66] are summarized in Table 4.

The SWRCs obtained for samples tend to have bimodal distributions once illustrated over the entire suction range. Hence, bi-modal SWRC equations proposed by Gitirana and Fredlund [66] were selected with the additional benefits of its clear physical meaning with independent properties. As described in Fredlund and Gitirana [66] degree of saturation,  $S$  mainly depends on nine parameters, which are the SWRC features for given suction,  $\psi$ .

$$S = f(\psi_{b1}, \psi_{res1}, S_{res1}, \psi_{b2}, S_b, \psi_{res2}, S_{res2}, a_b, S_{max}, \psi) \tag{6}$$

where  $\psi_b$  represents the air-entry suction of the drying SWRC or water-entry suction for wetting SWRC,  $\psi_{res}$  being the residual soil suction,  $S_{res}$  the residual degree of saturation, and  $a_b$  the sharpness of the transitions at bending points. The subscripts 1 and 2 denote the two levels of soil structures.  $S_b$  is the degree of saturation at the air-entry of the second structure level.  $S_{max}$  is maximum degree of

**Fig. 12** Soil water retention curves (SWRCs) for biochar amended soil and fitted with Gitirana and Fredlund equation

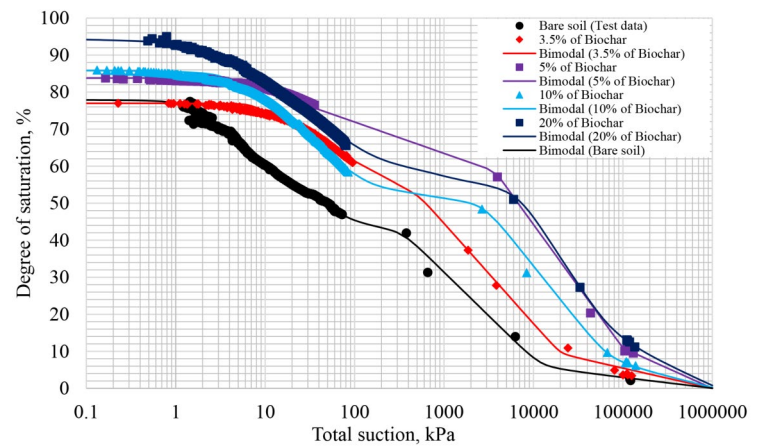


**Table 4** Gitirana and Fredlund's equation fitting parameters for biochar-amended soil

Bi-modal Fitting Parameters, Symbols	Description	Biochar amended soil				
		0	3.5%	5%	10%	20%
$a_b$	Sharpness of the transtistions (slope of SWRC)	0.02	0.02	0.025	0.03	0.06
$\psi_{b1}$ , kPa	1st air entry value (AEV)	1.2	4	4	4	4
$\psi_{res1}$ , kPa	1st residual soil suction	88	200	200	200	200
$S_{res1}$ (-)	1st residual degree of saturation	0.57	0.75	0.83	0.60	0.61
$\psi_{b2}$ , kPa	2nd air entry value (AEV)	340	550	2000	2800	7000
$S_b$ (-)	2nd degree of saturation	0.55	0.74	0.79	0.59	0.59
$\psi_{res2}$ , kPa	2nd residual soil suction	17,000	20,000	60,000	68,000	70,000
$S_{res2}$ (-)	2nd residual degree of saturation	0.07	0.12	0.13	0.10	0.13
$S_r^{max}$ (-)	Maximum degree of saturation (wetting)	0.780	0.770	0.838	0.860	0.950

saturation upon soaking the sample during wetting which can be less than 100%. Gitirana and Fredlund's formulation applies four hyperbolae to model the bimodal feature of SWRC in  $\log(\psi) - S$  coordinates. Their full descriptions are lengthy and thus omitted here for brevity. Table 4 summarizes the curve-fitting parameters for the SWRCs.

Figure 13 (a-i) illustrates the impact of varying biochar concentrations (0%, 3.5%, 5%, 10%, and 20%) on soil-water retention curve (SWRC) parameters of the Gitirana and Fredlund [66] model. The plots reveal insights into the alteration of soil properties. The sharpness of transitions (Fig. 13(a)), as reflected in the slope of the SWRC, exhibits a progressively increasing value with higher biochar content, reaching its peak at 0.06 for a 20% biochar concentration. The first-level air entry value suction (AEV), representing the suction at which air enters the macro soil-water system, is notably lower at 1.2 kPa for bare soil (0% biochar), while becoming higher at 4 kPa for biochar concentrations of 3.5%, 5%, 10%, and 20%. This implies a smaller maximum pore size with biochar inclusion. This observation seems counterintuitive at first, given the larger particle size of biochar (Fig. 2). However, the same explanation could be proposed as for the smaller permeability of BAS. The silty sand matrix in BAS would be of higher density than that of bare soil and thus of higher AEV suction at this first level.

The second AEV suction demonstrates a non-linear trend with biochar content, with a notable increase from 340 to 7000 kPa as the biochar concentration rises from 0 to 20%. This can be attributed to the increase in smaller intraparticle pores present in biochar mixture, resulting in higher air entry values in the second level of soil pores [67, 68]. In Fig. 13(c-d), the first residual soil suction stays about the same at 200 kPa for biochar concentrations of 3.5%, 5%, 10%, and 20%. For bare soil with no biochar, it shows a slightly lower value of 88 kPa. The increasing trend in the second residual soil suction, ranging from 17,000 to 70,000 kPa with rising biochar content, indicates a potential enhancement in the soil's ability to retain water. Examining the degree of saturation parameters in Fig. 13 (e-f) suggests the first residual degree of saturation peaks at 0.83 for 5% biochar, which indicates improved water retention after the first stage of drying. The fluctuations in the second degree of saturation and the second residual degree of saturation, particularly reaching a maximum of 0.13 for 5% biochar, suggest the intricate relationship between biochar content and the distribution of water within the soil matrix. Furthermore, the maximum degree of saturation (Fig. 13i) exhibits an ascending trend with biochar, reaching its peak at 0.950 for 20% biochar. This is expected to be related to the hydrophilicity trait observed in biochar which was not so well

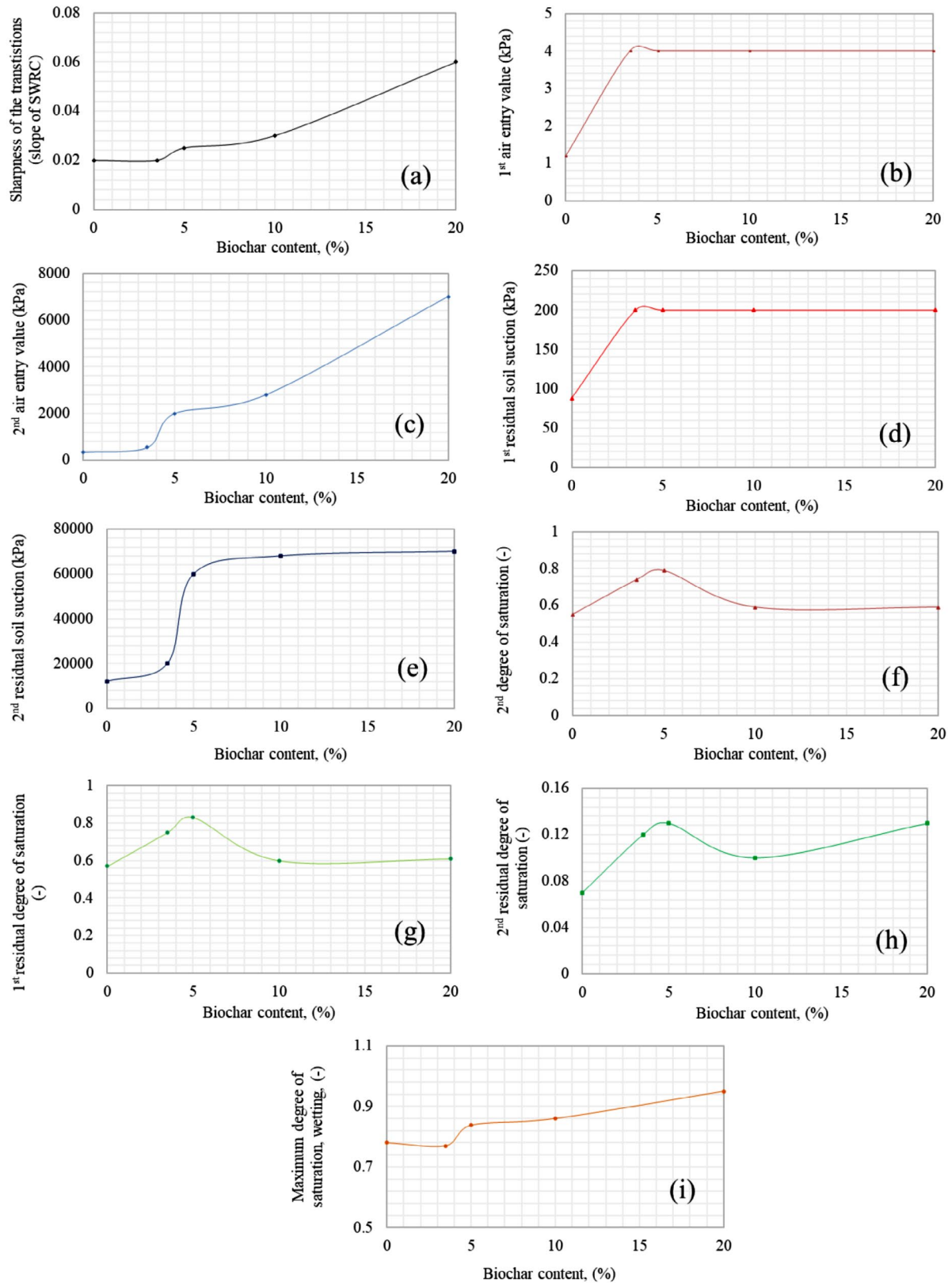


**Fig. 13** The influence of biochar on SWRC using Gitirana and Fredlund (2004) model: (a) sharpness of the transitions; (b) 1<sup>st</sup> air entry value (kPa); (c) 2<sup>nd</sup> air entry value (kPa); (d) 1<sup>st</sup> residual soil suction

(kPa); (e) 2<sup>nd</sup> residual soil suction (kPa); (f) 2<sup>nd</sup> degree of saturation (-); (g) 1<sup>st</sup> residual degree of saturation (-); (h) 2<sup>nd</sup> residual degree of saturation (-); (i) Maximum degree of saturation (-)

observed in the bare soil without biochar. In other words, the biochar inclusion could improve the hydrophilicity of the BAS and related to the higher maximum degree of saturation of the mixture in soaked condition.

### Effects of Biochar on Permeability (*k*) Functions

In Fig. 14, the effect of biochar on permeability (*k*) functions of silty sand (SM) with varying biochar contents

(3.5%, 5%, 10%, and 20%) is presented. Additionally, the saturated permeability ( $k_{sat}$ ), which was previously illustrated in Fig. 10 through conventional testing (falling-head permeability test), is included in the same graph, providing a reference  $k_{sat}$  value and conveniently plotted at a suction of 1 kPa for ease of comparison in logarithmic suction scale. To better compare the biochar influence, these plots are presented together in Fig. 15, using the curve-fitting equations of Gardner (1958), showing a reduction in permeability

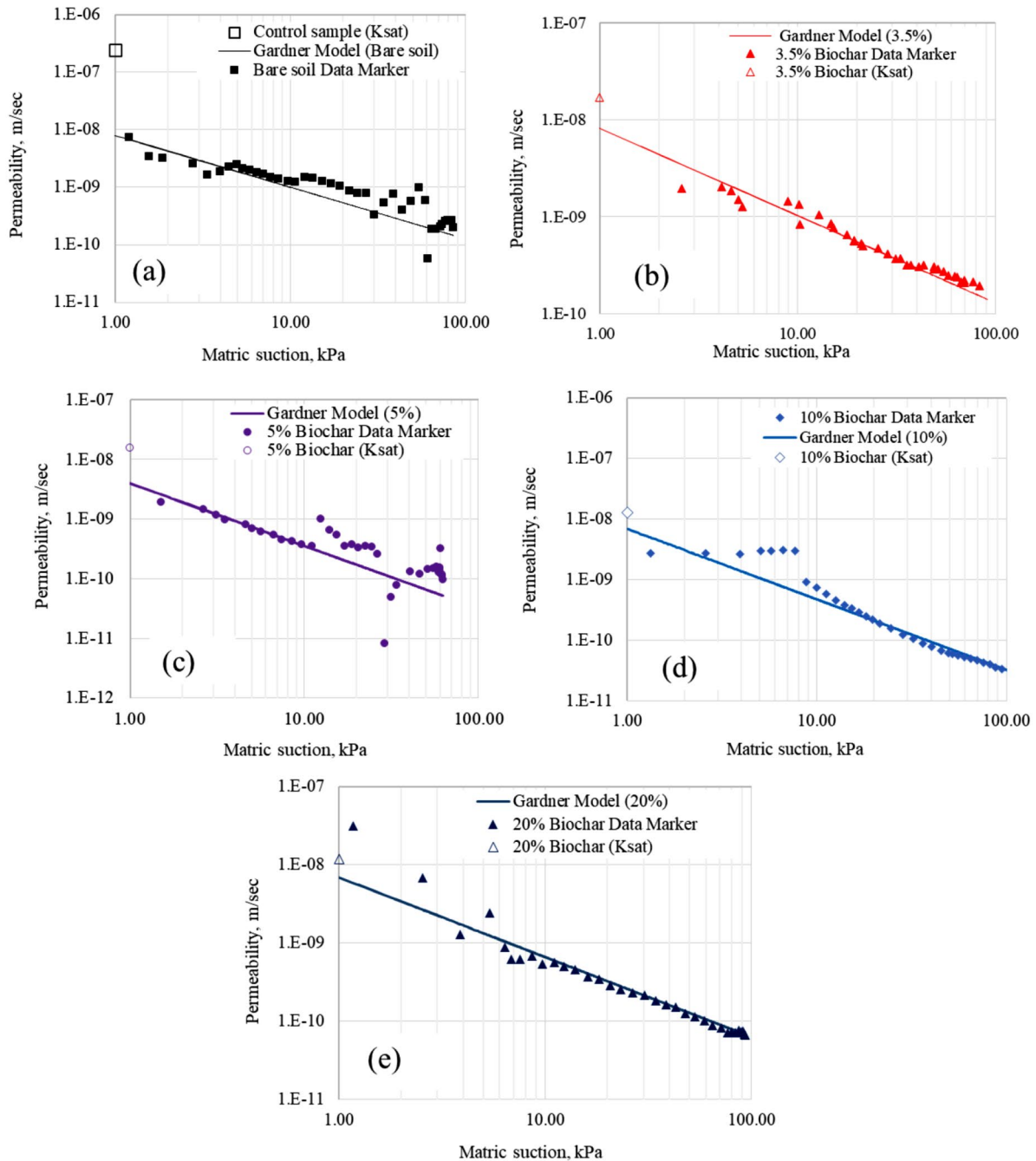


**Fig. 14** Permeability (*k*) functions for BAS: (a) bare soil; (b) 3.5% of biochar; (c) 5% of biochar; (d) 10% of biochar; (e) 20% of biochar

with increasing suction. It is well established that as suction in unsaturated soils increases, permeability decreases due to reduced water content, formation of water menisci, drainage of larger pores, and the dominance of film flow in smaller pores.

Notably, the 5% biochar-amended soil demonstrates the maximum reduction in unsaturated permeability when compared to other biochar concentrations. Further observations on the 3.5% biochar treatment exhibit a trend almost similar to the unamended soil, hinting at a potential threshold effect. In contrast, the 20% biochar-amended soil displays a smaller reduction in permeability compared to the 5% and 10% concentrations. This indicates that incorporating higher amounts of biochar into the soil can help reduce the unsaturated permeability until a certain threshold is reached where further biochar addition may not be as effective. The exact explanation for this threshold effect is currently unknown, but it is likely related to changes in the fabric of the biochar-amended soils and the distribution of interconnected water-filled voids. More detailed SEM studies are required to confirm this.

Another interesting trend in Fig. 15 is the difference difference between the unsaturated permeability ( $k$ ) from the instantaneous profile (IP) test at suction of 1 kPa and the  $k_{sat}$  values determined through conventional testing. The suction of about 1 kPa correspond to a degree of saturation between 77% (for bare soil) and 93% (for 20% biochar content) (see Fig. 12), indicating that the soil was nearly saturated and still of occluded air. The difference between  $k$  and  $k_{sat}$  values is attributed to a combination of factors. These include the permeability's dependency on positive pore pressure and effective stress, as documented in previous studies [69]. Moreover, it could be due to the lower

accuracy of permeability determined by the IP test at small suction [59] and the presence of air bubbles and their dissolution with testing time [43, 59].

### Relative Permeability

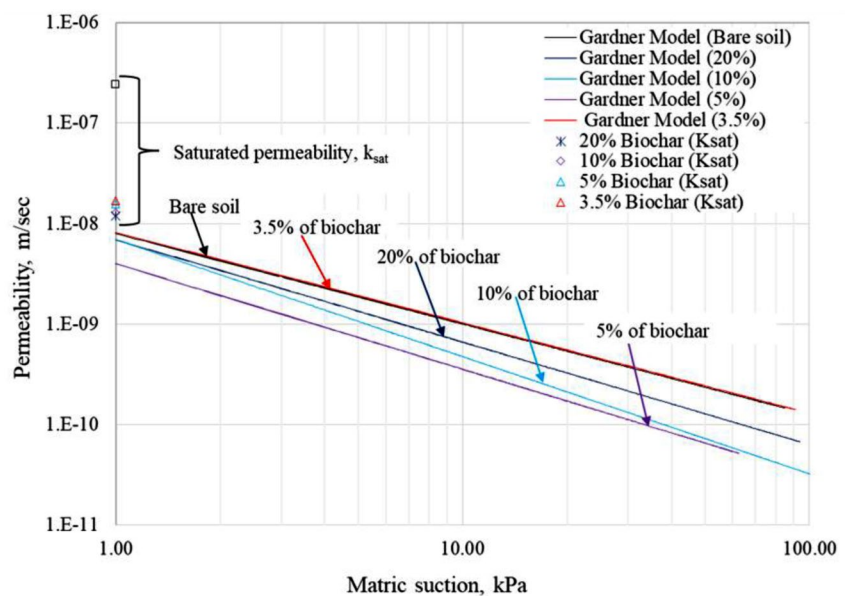
The study explores the influence of biochar on the relative permeability of residual silty sand (SM), utilizing the Gardner (1958) as shown in Eq. 7;

$$k(\psi) = \frac{k_{sat}}{1 + c_g \psi^{n_g}} \quad (7)$$

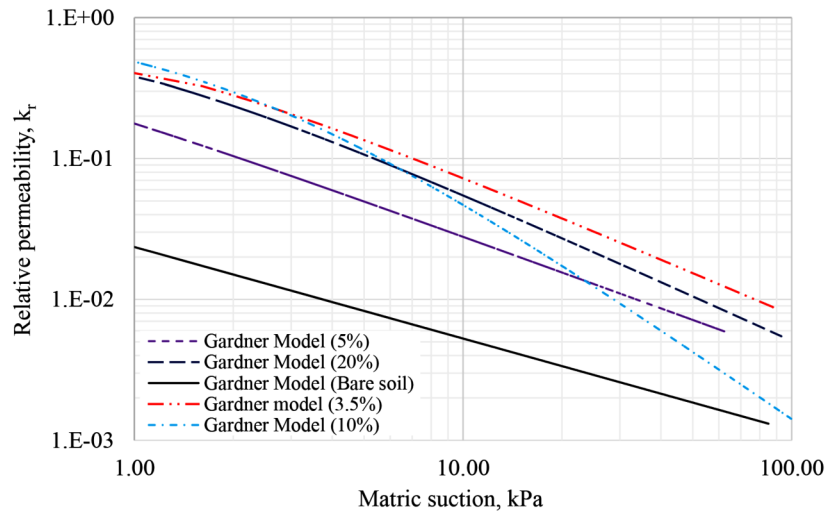
; where,  $\psi$  is suction (kPa),  $k_{sat}$  is the saturated permeability (m/s),  $k(\psi)$  is the permeability function (m/s) related to suction, and  $c_g$  (dimensionless) is the parameter related to the air entry value (AEV),  $n_g$  (dimensionless) parameter controls the subsequent slope of the decrease in conductivity with increasing suction. Figure 16 unveils a distinctive curve within the lower suction range (0.01 to 1 kPa), suggesting a potentially more sensitive response of permeability to changes in a lower range of suction. This nuanced behavior may be indicative of the soil's macro-pore structure. Beyond 1 kPa, Fig. 16 exhibits a pattern similar to Fig. 15, implying a consistent trend in permeability under higher suction conditions.

Table 5 shows the fitting parameters into these relationships, indicating that  $c_g$  values increase with higher concentrations of biochar, ranging from 0.003 for bare soil to 1.789 and 0.688 for soil with 10% and 20% of biochar respectively. Additionally,  $n_g$  values exhibit variation with biochar concentration, indicating a shift from 0.650 in unamended

**Fig. 15** Permeability ( $k$ ) functions of BAS fitted to Gardner's (1958) equation



**Fig. 16** Relative Permeability ( $k_r$ ) function for silty sand (SM) fitted to Gardner’s (1958) equation with BAS



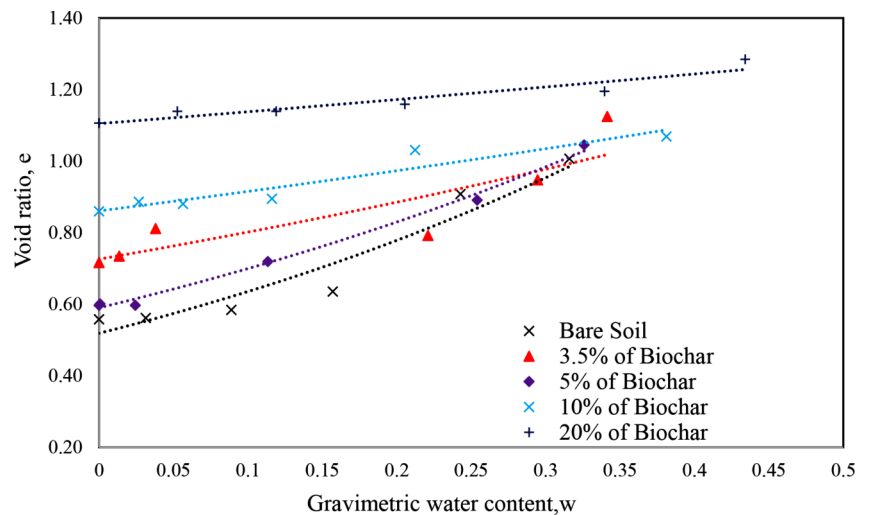
**Table 5** Gardner’s (1958) equation fitting parameters for biochar-amended soil

Concentrations of Biochar	Curve fitting parameters				RMSE	$R^2$
	$k_{sat}$ (m/s)	$C_g$	$n_g$			
0**	2.41E-07	0.003	0.650		2E-03	0.855
3.5%	1.69E-08	0.437	0.852		3E-04	0.654
5%	1.56E-08	0.150	0.850		3E-04	0.682
10%	1.27E-08	1.789	1.624		3E-03	0.897
20%	1.19E-08	0.688	1.060		2E-02	0.820

0\*\* = Control parameter (Bare soil),  $k_{sat}$  = saturated permeability (m/sec),

RMSE = root mean square error

**Fig. 17** Effect of biochar on volume change of silty sand



soil to 1.624 and 1.060 in soil with 10% and 20% biochar respectively.

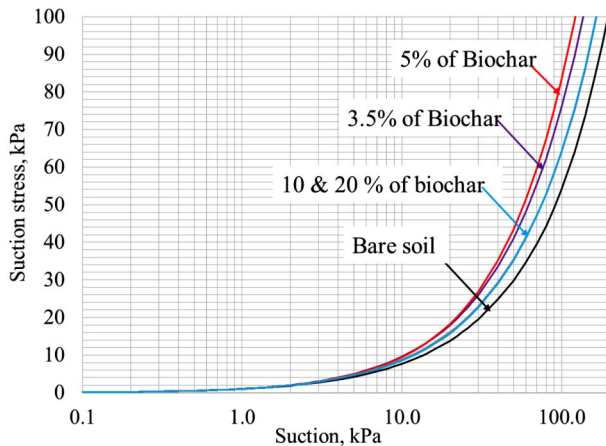
**Effect of Biochar on Soil Volume Change**

Figure 17 shows the impact of varying biochar concentrations on void ratio,  $e$ , and gravimetric water content,  $w$ , during drying. Table 6 shows the curve fitting equations of the observed trend. As biochar concentration increases, the

maximum void ratio and water content increase due to the higher porous structure as explained earlier. The decrease in void ratio with decreasing water content suggest the potential amount of desiccation volume change experienced by the soil during drought period. A smaller reduction in void ratio of the biochar-soil mixture at 20%  $B_c$  is evident, with an equivalent volumetric strain of 7.8% upon drying as compared to the volumetric strain of 22.1% for bare soil. This clearly indicates that the biochar could be used as a soil

**Table 6** The equations for curve fitting parameters for biochar-amended soil

Biochar concentration, %	Equation	$R^2$
0 (bare soil)	$y = 0.5187e^{2.03x}$	0.936
3.5	$y = 0.726e^{0.9908x}$	0.773
5	$y = 0.5899e^{1.705x}$	0.994
10	$y = 0.8609e^{0.6128x}$	0.899
20	$y = 1.1048e^{0.2956x}$	0.897

**Fig. 18** Effect of biochar on suction stress characteristic curve

amendment to alleviate the volume change problem and the desiccation crack of unsaturated soil.

## Engineering and Environmental Benefits

### Enhancement of Suction Stress

Suction stress ( $\sigma^s$ ) in unsaturated soils [71] is a macroscopic stress arising from interparticle forces at or near contacts, including physicochemical, cementation, surface tension forces, and negative pore-water pressure. Suction stress contributes to enhancement of shear strength through such interparticle forces and bonding. Jotisankasa & Mairaing [61] suggested an estimation of the suction stress based on the soil-water retention curve (SWRC) as follows:

$$\sigma^s = \frac{\theta - \theta_r}{\theta_s - \theta_r} \times (u_a - u_w) \quad (8)$$

where  $\theta$  is volumetric water content;  $\theta_s$  is saturated volumetric water content;  $\theta_r$  is residual volumetric water content; and  $u_a$  and  $u_w$  are pore-water and pore air pressures. The observed SWRC was then used to estimate the variation of suction stress with suction as shown in Fig. 18. It is evident that there is enhancement of suction stress in soils with 3.5% and 5% biochar, attributed to the porous structure of biochar creating microsities that enhance capillary forces.

Since suction stress is theoretically the product of the normalized water content ( $\frac{\theta - \theta_r}{\theta_s - \theta_r}$ ) and suction, an increase in suction stress at any given suction for 5% biochar is caused by enhanced water retention capability and a corresponding rise in the normalized water content. However, for higher biochar percentages (20%), a minor increment in suction stress is noted, likely due to the corresponding increase in residual volumetric water content of the higher biochar level that could reduce the normalized water content used to calculate suction stress, hence causing a slower rate of suction stress increase. This nuanced relationship demonstrates the importance of carefully optimizing biochar levels in soil to improve the suction stress. However, the observation is not conclusive and still requires further experimental validation.

### Removal of CO<sub>2</sub>

In Fig. 19, the potential benefit of biochar-amended soil for carbon dioxide (CO<sub>2</sub>) removal is illustrated. As a first estimate, an analysis was made based on the assumption that 1 kg of biochar can sequester 1.9 kg of CO<sub>2</sub> based on previous studies [72, 73]. The concentration of biochar in the soil, together with the thickness of the soil layer were used to calculate the resulting potential CO<sub>2</sub> removal. At a 3.5% biochar concentration, the CO<sub>2</sub> removal increases with increasing soil thickness, ranging from 0.39 kg at 0.5 cm to 7.73 kg at 10 cm. Similarly, for a 5% biochar concentration, the emissions exhibit a proportional increase, varying from 0.53 to 10.58 kg across the same range of soil thickness. This kind of plot would be useful for geotechnical engineers to justify the benefit of biochar application not only based on improvement in geotechnical performance but also on the environmental benefit in terms of carbon sink.

### Water Storage Capacity

Water storage capacity in soil refers to the maximum water content a soil can hold before it drains downward and approximated as its field capacity ( $FC$ ), which is the water content after free or gravity drainage. Field capacity is often arbitrarily reported as the water content at suction of 33 kPa [53, 74, 75]. Figure 11 was used to determine the volumetric water content ( $\theta$ ) at the field capacity and then the storage capacity ( $SC$ ) of a soil layer can be determined by integrating its volumetric water content ( $\theta$ ) over its thickness ( $b_t$ ). Assuming a constant field capacity, the water storage capacity for a simple soil cover can be described by

$$SC = \int_0^{b_t} \theta dz = (FC) b_t \quad (9)$$



**Fig. 19** Potential CO<sub>2</sub> emission reduction for different thickness of biochar application assuming an average of 1.9 mt CO<sub>2</sub> removed per mt of biochar

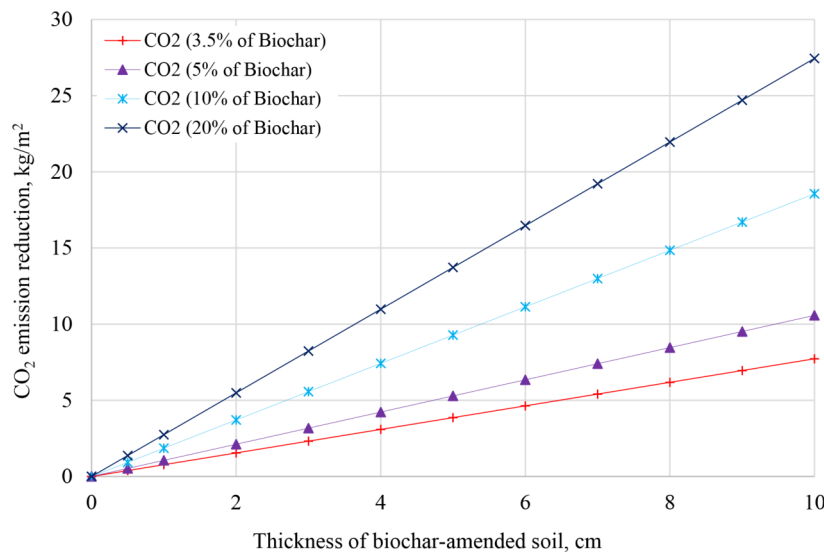


**Fig. 20** Field water storage capacity of biochar amended soil

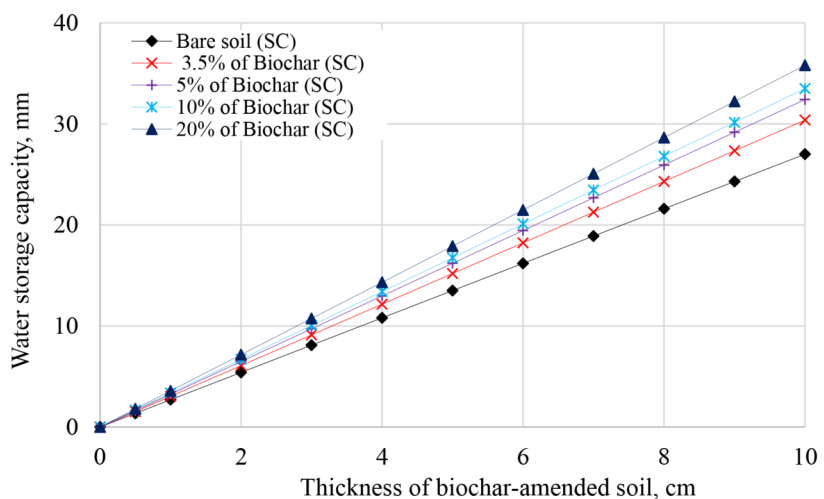


Figure 20 show the data on water storage capacity (*SC*) of soil at varying thicknesses and different percentages of biochar amendment. It provides valuable insights into the potential benefits of biochar in enhancing soil’s water retention capabilities. As observed, the addition of biochar significantly increases the water storage capacity compared to bare soil. At a 3.5% biochar concentration, the soil exhibits a noticeable improvement in its ability to hold water, which becomes more pronounced as soil thickness increases. The trend continues with 5% biochar, 10% biochar, and 20% biochar amendments, with the highest biochar concentration resulting in the most substantial water storage capacity.

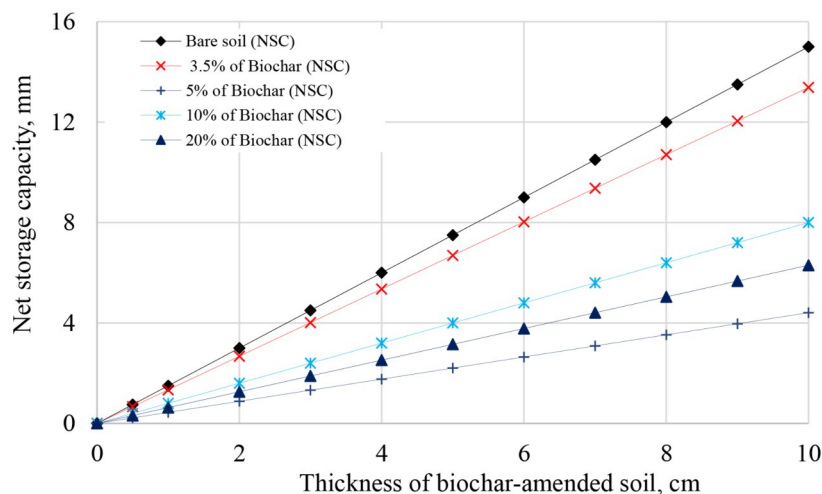
The data on net storage capacity (*NSC*) in relation to biochar concentration and soil thickness provides another outlook. The *NSC*, often referred to as the available water capacity, is calculated based on the difference between the field capacity (*FC*) and the permanent wilting point (*PWP*)

of the soil over its thickness (*b<sub>t</sub>*). The *PWP* is typically defined as the water content at a suction head of 150 m [76, 77]. The net storage capacity (*NSC*) of a soil layer can be approximated by Eq. 10.

$$NSC = (FC - PWP) b_t \tag{10}$$

Surprisingly, the result in Fig. 21 suggests a counterintuitive trend where increasing biochar concentrations leads to a significant reduction in the soil’s *NSC* as soil thickness, *b<sub>t</sub>*, increases. The plausible explanation for this phenomenon lies in the effect of biochar on the volumetric water content ( $\theta$ ) in the soil at the *PWP*. It appears that the addition of biochar results in higher  $\theta$  levels at the 150 m suction head, effectively causing the *PWP* to rise, which reduces the net storage capacity of water. On the other hands, the higher *PWP* of biochar-soil mixture implies improved

**Fig. 21** Net storage capacity (NSC) of water of biochar amended soil



water availability for plants in severe drought conditions, emphasizing the potential benefits of biochar supporting plant resilience in bioengineering application. Nevertheless, Philip [75] and Raats et al. [77] emphasize the complexity of the wilting point in soil and warns against using the wilting point as a fixed index for soil moisture availability due to its potential for misleading conclusions. This observation warrants further studies by using numerical analysis and field trial to validate this.

## Conclusions

This study investigated the effects of biochar amendment on key hydraulic properties of tropical residual silty sand with varying biochar concentrations (3.5%, 5%, 10%, and 20% by weight). The following conclusions can be made based on the findings from this study.

- The addition of biochar led to an increase in volumetric water content by about 8 to 10% for the suction range between zero and 100 kPa as compared to bare soil. This reflects the intraparticle voids and porosity of the biochar particles which improve the water retention of the BAS. However, the effect was less pronounced if the biochar percentage was less than 3.5% by weight especially for suction lower than 5 kPa.
- The soil-water retention curves (SWRCs) of the BAS had bimodal shape. Their curve fitting parameters tended to non-linearly increase with biochar percentage, including sharpness of the transitions; 1st and 2nd air entry suctions, 1st and 2nd residual soil suctions, 1st and 2nd maximum degrees of saturation and 1st and 2nd residual degrees of saturation.

- An increase in biochar percentage of 20% brought about a significant reduction in saturated permeability ( $k_{sat}$ ) by about 20 times, despite an increase in void ratio of the BAS with biochar. The same trend is also observed in unsaturated permeability ( $k$ ) functions at a given suction value and overall density. The observed phenomenon can be attributed to the abundant intraparticle pores found within the biochar structure and likely reduction of interconnected pores in BAS matrix, as well as the presence of hydrophobic and hydrophilic functional groups on the surface of the biochar.
- The biochar addition led to reduction in volume change upon drying. The biochar-soil mixture at 20% biochar ( $B_c$ ) showed a smaller reduction in void ratio, with a volumetric strain of 7.8% upon drying, compared to 22.1% for bare soil.
- The theoretical variation of suction stress predicted using SWRC indicated that BAS with 3.5% and 5% biochar had enhanced suction stress due to biochar's porous structure, while at higher biochar percentages (10% and 20%), only a minor increase in suction stress was predicted.
- This study also highlighted the environmental benefits of biochar as a carbon sink and discussed the water storage capacity of the BAS cover system, indicating a need for further research in these areas.

**Acknowledgements** The first author is grateful to the scholarship provided by the Department of Civil Engineering and Faculty of Engineering, Kasetsart University. Valuable assistance provided by the students and staffs at Geotechnical division of Department of Civil Engineering, Department of Soil Physics, Kasetsart University and Green Ground Solutions, co. Ltd is gratefully acknowledged. Additionally, they express their gratitude for the generous provision of the WP4C equipment, made possible through JICA/JST's SATREPS project from Japan in 2023.

**Data Availability** Data will be made available upon reasonable request.

## Declarations

**Ethics Approval and Consent to Participate** All authors contributed to the study conception and design. Material preparation, data collection and analysis were performed by first author and second author. The first draft of the manuscript was written by first author under the guidance of second author and all authors edited and commented on previous versions of the manuscript. All authors read and approved the final manuscript.

**Conflict of Interest** The authors have no financial or proprietary interests in any material discussed in this article.

## References

- Reubens B, Poesen J, Danjon F, Geudens G, Muys B (2007) The role of fine and coarse roots in shallow slope stability and soil erosion control with a focus on root system architecture: a review. *Trees* 21(4):385–402
- Montgomery DR (2007) Soil erosion and agricultural sustainability. *Proceedings of the National Academy of Sciences*, 104(33): 13268–13272
- Kumar H, Ganesan SP, Bordoloi S, Sreedeeep S, Lin P et al (2019) Erodibility assessment of compacted biochar amended soil for geo-environmental applications. *Sci Total Environ* 672:698–707
- Jotisankasa A, Sawangsuriya A, Muanlhao T, Nishimura S (2023) Application of nature-based solution for resilient and sustainable slopes in Thailand. *Proceedings of Asia Australia Road Conference*. Advanced Technology Implementation Towards Sustainable Road Development. 24–27 August 2023, Labuan Bajo, Indonesia
- Schmidt KM, Roering JJ, Stock JD, Dietrich WE, Montgomery DR et al (2001) The variability of root cohesion as an influence on shallow landslide susceptibility in the Oregon Coast Range. *Can Geotech J* 38(5):995–1024
- Ng CWW, Leung AK, Woon KX (2014) Effects of soil density on grass-induced suction distributions in compacted soil subjected to rainfall. *Can Geotech J* 51(3):311–321
- Sadasivam BY, Reddy KR (2015) Adsorption and transport of methane in landfill cover soil amended with waste-wood biochars. *J Environ Manage* 158:11–23
- Jayawardhana Y, Kumarathilaka P, Herath I, Vithanage M (2016) Municipal solid waste biochar for prevention of pollution from landfill leachate. *Environmental materials and waste*. Academic, pp 117–148
- Ni JJ, Chen XW, Ng CWW, Guo HW (2018) Effects of biochar on water retention and matric suction of vegetated soil. *Géotechnique Lett* 8(2):124–129
- Weber K, Quicker P (2018) Properties of biochar. *Fuel* 217:240–261
- Wong JTF, Chen Z, Chen X, Ng CWW, Wong MH (2017) Soil-water retention behavior of compacted biochar-amended clay: a novel landfill final cover material. *J Soils Sediments* 17(3):590–598
- Wong JTF, Chen Z, Wong AYY, Ng CWW, Wong MH (2018) Effects of biochar on hydraulic conductivity of compacted kaolin clay. *Environ Pollut* 234:468–472
- Garg A, Hazra B, Zhu H, Wen Y (2019) A simplified probabilistic analysis of water content and wilting in soil vegetated with non-crop species. *CATENA* 175:123–131
- Joseph S, Peacocke C, Lehmann J, Munroe P (2012) Developing a biochar classification and test methods. *Biochar for environmental management*. Routledge, pp 139–158
- Sohi SP, Krull E, Lopez-Capel E, Bol R (2010) A review of biochar and its use and function in soil. *Adv Agron* 105:47–82
- Kookana RS, Sarmah AK, Van Zwieten L, Krull E, Singh B (2011) Biochar application to soil: agronomic and environmental benefits and unintended consequences. *Adv Agron* 112:103–143
- Abel S, Peters A, Trinks S, Schonsky H, Facklam M et al (2013) Impact of biochar and hydrochar addition on water retention and water repellency of sandy soil. *Geoderma* 202–203:183–191
- Karhu K, Mattila T, Bergström I, Regina K (2011) Biochar addition to agricultural soil increased CH<sub>4</sub> uptake and water holding capacity – results from a short-term pilot field study. *Agric Ecosyst Environ* 140(1–2):309–313
- Chen B, Yuan M, Qian L (2012) Enhanced bioremediation of PAH-contaminated soil by immobilized bacteria with plant residue and biochar as carriers. *J Soils Sediments* 12(9):1350–1359
- Yu L, Tang J, Zhang R, Wu Q, Gong M (2012) Effects of biochar application on soil methane emission at different soil moisture levels. *Biol Fertil Soils* 49(2):119–128
- Yu O-Y, Raichle B, Sink S (2013) Impact of biochar on the water holding capacity of loamy sand soil. *Int J Energy Environ Eng* 4(1):44
- Ulyett J, Sakrabani R, Kibblewhite M, Hann M (2013) Impact of biochar addition on water retention, nitrification and carbon dioxide evolution from two sandy loam soils. *Eur J Soil Sci* 65(1):96–104
- Reddy KR, Yaghoubi P, Yukselen-Aksoy Y (2015) Effects of biochar amendment on geotechnical properties of landfill cover soil. *Waste Manage Research: J Sustainable Circular Econ* 33(6):524–532
- Waqas M, Li G, Khan S, Shamshad I, Reid BJ et al (2015) Application of sewage sludge and sewage sludge biochar to reduce polycyclic aromatic hydrocarbons (PAH) and potentially toxic elements (PTE) accumulation in tomato. *Environ Sci Pollut Res* 22(16):12114–12123
- Rodríguez-Vila A, Selwyn-Smith H, Enunwa L, Smail I, Covelo EF et al (2017) Predicting Cu and Zn sorption capacity of biochar from feedstock C/N ratio and pyrolysis temperature. *Environ Sci Pollut Res* 25(8):7730–7739
- Uzoma KC, Inoue M, Andry H, Zahoor A, Nishihara E (2011) Influence of biochar application on sandy soil hydraulic properties and nutrient retention. *J Food Agric Environ* 9(3/4 part 2):1137–1143
- Ahmad M, Rajapaksha AU, Lim JE, Zhang M, Bolan N et al (2014) Biochar as a sorbent for contaminant management in soil and water: a review. *Chemosphere* 99:19–33
- Haefele SM, Konboon Y, Wongboon W, Amarante S, Maarifat AA, Pfeiffer EM, Knoblauch CJ, F.C.R (2011) Effects and fate of biochar from rice residues in rice-based systems. *Field Crops Res* 121(3):430–440
- Kuzyakov Y, Bogomolova I, Glaser B (2014) Biochar stability in soil: decomposition during eight years and transformation as assessed by compound-specific <sup>14</sup>C analysis. *Soil Biol Biochem* 70:229–236
- Singh BP, Cowie AL, Smernik RJ (2012) Biochar carbon stability in a clayey soil as a function of feedstock and pyrolysis temperature. *Environ Sci Technol* 46(21):11770–11778
- Lal R (2015) Sequestering carbon and increasing productivity by conservation agriculture. *J Soil Water Conserv* 70(3):55A–62A
- Brassard P, Godbout S, Raghavan V (2016) Soil biochar amendment as a climate change mitigation tool: key parameters and mechanisms involved. *J Environ Manage* 181:484–497

33. Baldock JA, Smernik RJ (2002) Chemical composition and bio-availability of thermally altered *Pinus resinosa* (Red pine) wood. *Org Geochem* 33(9):1093–1109
34. Wang Z, Zheng H, Luo Y, Deng X, Herbert S, Xing B (2013) Characterization and influence of biochars on nitrous oxide emission from agricultural soil. *Environ Pollut* 174:289–296
35. Sohi SP (2012) Carbon storage with benefits. *Science* 338(6110):1034–1035
36. Woolf D, Amonette JE, Street-Perrott FA, Lehmann J, Joseph S (2010) Sustainable biochar to mitigate global climate change. *Nature communications*, 1(1), p.56
37. Fredlund DG, Rahardjo H (1993) *Soil mechanics for unsaturated soils*. Wiley
38. Tamari S, Bruckler L, Halbertsma J, Chadoeuf J (1993) A simple method for determining Soil Hydraulic properties in the Laboratory. *Soil Sci Soc Am J* 57(3):642–651
39. Huat BB, Ali FH, Mariappan S (2005) Effect of surface cover on water infiltration rate and stability of cut slope in residual soils. *Electron J Geotech Eng*, 10
40. Huat BB, Ali FH, Low TH (2006) Water infiltration characteristics of unsaturated soil slope and its effect on suction and stability. *Geotech Geol Eng* 24:1293–1306
41. Rahardjo H, Satyanaga A, Mohamed H, Yee Ip SC, Shah RS (2018) Comparison of soil–water characteristic curves from conventional testing and combination of small-scale centrifuge and dew point methods. *Geotech Geol Eng* 37(2):659–672
42. Leung AK, Coo JL, Ng CWW, Chen R (2016) New transient method for determining soil hydraulic conductivity function. *Can Geotech J* 53(8):1332–1345
43. Jotisankasa A, Sirirattanachai T (2017) Effects of grass roots on soil-water retention curve and permeability function. *Can Geotech J* 54(11):1612–1622
44. Ng CW, Pang YW (2000) Experimental investigations of the soil-water characteristics of a volcanic soil. *Can Geotech J* 37(6):1252–1264
45. Downie A, Crosky A, Munroe P (2009) *Physical properties of biochar: Biochar for environment management science and technology*. Earthscan, London
46. Lei O, Zhang R (2013) Effects of biochars derived from different feedstocks and pyrolysis temperatures on soil physical and hydraulic properties. *J Soils Sediments* 13(9):1561–1572
47. Nimmo JR (2004) Porosity and pore size distribution. *Encyclopedia Soils Environ* 3(1):295–303
48. Verheijen F, Jeffery S, Bastos AC, Van der Velde M, Diafas I (2010) Biochar application to soils. *Crit Sci Rev Eff soil Prop Processes Funct EUR* 24099(162):2183–2207
49. Gao X, Masiello CA (2017) 12 Analysis of biochar porosity by pycnometry. *Biochar: A Guide to Analytical Methods*, p.132
50. Eden M, Gerke HH, Houot S (2017) Organic waste recycling in agriculture and related effects on soil water retention and plant available water: a review. *Agron Sustain Dev* 37(2). <https://doi.org/10.1007/s13593-017-0419-9>
51. Wall DK, Zeiss C (1995) Municipal landfill biodegradation and settlement. *J Environ Eng* 121(3):214–224
52. Paetsch L, Mueller CW, Kögel-Knabner I, Von Lütow M, Girardin C, Rumpel C (2018) Effect of in-situ aged and fresh biochar on soil hydraulic conditions and microbial C use under drought conditions. *Sci Rep* 8(1):6852
53. Jotisankasa A, Tapparnich J, Booncharoenpanich P, Hunsachainan N, Soralump S (2010) Unsaturated soil testing for slope studies. In *Proc. Int. Conf. on Slope. Thailand*
54. Adeniyi AG, Iwuozor KO, Muritala KB, Emenike EC, Adeleke JA (2023) Conversion of biomass to biochar using top-lit updraft technology: a review. *Biofuels Bioprod Biorefin* 17(5):1411–1424. <https://doi.org/10.1002/bbb.2497>
55. Warm H Worldwide, n.d. How to Make a Biochar Machine – TLUD. Retrieved from <https://www.warmheartworldwide.org/biochar-training-resources.html>
56. Barnes RT, Gallagher ME, Masiello CA, Liu Z, Dugan B (2014) Biochar-Induced Changes in Soil Hydraulic Conductivity and Dissolved Nutrient Fluxes Constrained by Laboratory Experiments. (Z. Zhou, Ed.) *PLoS ONE*, 9(9): e108340
57. Mairiang W, Jotisankasa A, Soralump S (2012) Some applications of unsaturated soil mechanics in Thailand: an appropriate technology approach. *Geotech Eng J SEAGS AGSSEA* 43(1):1–11
58. Jotisankasa A, Porlila W, Soralump S, Mairiang W (2007) April. Development of a low-cost miniature tensiometer and its applications. In *Proceedings of 3rd Asian Conference on Unsaturated Soils UNSATASIA 2007* (pp. 475–480). Science Press, Nanjing, China
59. Peters A, Durner W (2008) Simplified evaporation method for determining soil hydraulic properties. *J Hydrol* 356(1–2):147–162
60. Jotisankasa A, Mahannopkul K, Sawangsuriya A (2015) Slope Stability and Pore-Water Pressure Regime in Response to Rainfall: a Case Study of Granitic Fill Slope in Northern Thailand. *Geotechnical Engineering Journal of the SEAGS & AGSSEA Vol. 46 No.1 March 2015 ISSN 0046-5828*. pp. 45–54
61. Jotisankasa A, Mairiang W (2010) Suction-monitored direct shear testing of residual soils from landslide-prone areas, *Journal of Geotechnical and Geoenvironmental Engineering*, ASCE, Vol. 136, No. 3, March 1, 2010
62. Ridley AM, Burland JB (1993) A new instrument for the measurement of soil moisture suction. *Géotechnique* 43(2):321–324
63. Fredlund DG, Rahardjo H, Fredlund MD (2012) *Unsaturated soil mechanics in Engineering Practice*. Wiley
64. Suliman W, Harsh JB, Abu-Lail NI, Fortuna A-M, Dallmeyer I et al (2017) The role of biochar porosity and surface functionality in augmenting hydrologic properties of a sandy soil. *Sci Total Environ* 574:139–147
65. Zhai Q, Rahardjo H (2012) Determination of soil-water characteristic curve variables. *Comput Geotech* 42:37–43. <https://doi.org/10.1016/j.compgeo.2011.11.010>
66. de Gitirana Jr FN, G., Fredlund DG (2004) Soil-water characteristic curve equation with independent properties. *J Geotech GeoEnviron Eng* 130(2):209–212
67. Chen R, Huang JW, Chen ZK, Xu Y, Liu J, Ge YH (2019) Effect of root density of wheat and okra on hydraulic properties of an unsaturated compacted loam. *Eur J Soil Sci* 70(3):493–506
68. Chen Z, Kamchoom V, Chen R, Prasittisopin L (2023) Investigating the impacts of Biochar Amendment and Soil Compaction on Unsaturated Hydraulic properties of Silty Sand. *Agronomy* 13(7):1845
69. Leroueil S, Hight DW (2013) Compacted soils: from physics to hydraulic and mechanical behaviour. *Adv Unsaturated Soils*, 41–59
70. Peters, A., & Durner, W., (2008) Simplified evaporation method for determining soil hydraulic properties. *Journal of Hydrology*, 356(1–2):147–162
71. Lu N, Likos WJ (2006) Suction stress characteristic curve for Unsaturated Soil. *J Geotech GeoEnviron Eng* 132(2):131–142
72. Woolf D, Amonette JE, Street-Perrott FA, Lehmann J, Joseph S (2010) Sustainable biochar to mitigate global climate change. *Nat Commun* 1(1). <https://doi.org/10.1038/ncomms1053>
73. *Global Biochar Market Report* (2023) International Biochar Initiative
74. Cassel DK, Nielsen DR (1986) Field capacity and available water capacity. *Methods soil Analysis: Part 1 Phys Mineralogical Methods* 5:901–926
75. Philip JR (1957) The physical principles of soil water movement during the irrigation cycle

76. Jury WA, Gardner WR, Gardner WH (1991) Soil physics. 5th Edition, John Wiley and Sons, New York, 122–123
77. Raats PA, Smiles DE, Warrick AW (2002) Contributions to environmental mechanics: introduction. Wash DC Am Geophys Union Geophys Monogr Ser 129:1–28

Springer Nature or its licensor (e.g. a society or other partner) holds exclusive rights to this article under a publishing agreement with the author(s) or other rightsholder(s); author self-archiving of the accepted manuscript version of this article is solely governed by the terms of such publishing agreement and applicable law.

**Publisher's Note** Springer Nature remains neutral with regard to jurisdictional claims in published maps and institutional affiliations.